All Optical Switching With a Single Quantum Dot Strongly Coupled to a Photonic Crystal Cavity

Arka Majumdar, Michal Bajcsy, Dirk Englund, and Jelena Vučković

***Abstract*—We theoretically analyze the optical nonlinearity present at very low optical power in a system consisting of a quantum dot strongly coupled to a cavity, and show that this system can be used for ultralow power and high-speed all-optical switching. We also present numerical simulation results showing both the detailed temporal behavior of such switch and the time-integrated energy transmission through the cavity. We use two different approaches—a quantum optical one and a semiclassical one—to describe the system's behavior, and observe reasonable agreement between the outcomes of numerical simulations based on these two approaches.**

***Index Terms*—All-optical switch, photonic crystal cavity, quantum dot (QD).**

I. Introduction

OPTICAL nonlinearity observable with low power light is a necessary requirement for efficient all-optical switching. Though cavities can be used to enhance the bulk optical nonlinearity of a material, the enhancement is often not sufficient for operation of a practical device. In recent years, several experiments have demonstrated optical nonlinearities at single photon, showing potential for implementation of ultralow power and high-speed all-optical gates and switches for classical information processing [1]–[4]. In particular, solid-state systems consisting of a single quantum dot (QD) strongly coupled to a nanocavity [2] are considered a highly promising candidate for such applications. The advantages of these systems include their small footprint and compatibility with standard nanofabrication procedures, in addition to an optical nonlinearity that is, in the ideal limit, observable with a single photon. Several experiments in recent years focused on probing of this optical nonlinearity and proposed its application for all-optical switching [5], [6]. In this paper, we provide a complete quantum optical description and a numerical simulation of the behavior of such all-optical switch. We also introduce a less computationally intensive semiclassical description, and find reasonable agreement between these two approaches.

Manuscript received December 31, 2011; revised March 20, 2012; accepted May 6, 2012. This work was supported by the Office of Naval Research through PECASE Award (supervised by Dr. C. Baatar), the National Science Foundation, and the Army Research Office. In addition, the National Science Foundation also supported this work performed in part at the Stanford Nanofabrication Facility of the National Nanotechnology Infrastructure Network. The work of D. Englund was supported by the Sloan Research Fellowship and the U.S. Air Force Office of Scientific Research Young Investigator Program under Grant FA9550-11-1-0014 (supervised by Dr. G. Pomrenke). This work was performed at E. L. Ginzton Laboratory, Stanford University, Stanford, CA.

A. Majumdar, M. Bajcsy, and J. Vučković are with Stanford University, Stanford, CA 94305 USA (e-mail: arkam@stanford.edu; bajcsy@stanford.edu; jela@stanford.edu).

D. Englund was with Stanford University, Stanford, CA 94305 USA. He is now with Columbia University, New York, NY 10027 USA (e-mail: englund@columbia.edu).

Digital Object Identifier 10.1109/JSTQE.2012.2202093

II. Quantum Optical Analysis

In this section, we provide a detailed quantum optical treatment of a strongly coupled QD-cavity system. The analysis is relevant for any single-mode cavity, and does not involve any typical characteristics of the photonic crystal. The Hamiltonian $\mathcal{H}$ describing the dynamics of the coupled system is given by

$$\mathcal{H} = \hbar\omega_d\sigma^\dagger\sigma + \hbar\omega_c a^\dagger a + \hbar g(a + a^\dagger)(\sigma + \sigma^\dagger) \tag{1}$$

where ω_c and ω_d are, respectively, the resonance frequencies of the cavity and the QD, a is the annihilation operator for the cavity mode, σ is the lowering operator for the QD and is denoted as $\sigma = |g\rangle\langle e|$ with $|e\rangle$ and $|g\rangle$ being the excited and the ground state of the QD, respectively, g is the coherent interaction strength between the QD and the cavity and is equal to the half of the vacuum Rabi splitting. This Hamiltonian can be solved to find the eigenenergies of the system. With a detuning δ between the QD and the cavity, the eigenenergies of the system are

$$E_\pm = \hbar(n+1)\omega_c + \hbar\frac{\delta}{2} \pm \frac{\hbar}{2}\sqrt{4g^2(n+1) + \delta^2}. \tag{2}$$

At zero detuning δ, the eigenenergies become $\hbar\omega_c \pm \hbar g\sqrt{n+1}$, where n is the number of excitations (photons) in the system. Generally, the system is probed with very weak laser, and hence, only the lower manifolds are populated. Considering only the first manifold ($n = 0$), the eigenenergies of the coupled system are $\hbar\omega_c \pm \hbar g$, whereas the eigenenergy the empty cavity is at $\hbar\omega_c$.

When this system is coherently driven by a laser with frequency ω_l and power P and incident onto the cavity, the overall Hamiltonian becomes

$$\mathcal{H}_d = \mathcal{H} + \hbar\mathcal{E}\sqrt{\kappa}(ae^{i\omega_l t} + a^\dagger e^{-i\omega_l t}) \tag{3}$$

where $\mathcal{E} = \sqrt{\frac{P}{2\hbar\omega_c}}$.

The interaction term $g(a + a^\dagger)(\sigma + \sigma^\dagger)$ in the Hamiltonian can be simplified to $g(a^\dagger\sigma + a\sigma^\dagger)$ by neglecting the terms $a^\dagger\sigma^\dagger$ and $a\sigma$ by rotating wave approximation (valid when the actual energies of the system, i.e., $\hbar\omega_c$ and $\hbar\omega_a$, are much greater than the coupling strength $\hbar g$). This approximation holds well in the optical system considered here, where the optical frequencies are $\sim$100 THz, whereas the coupling strength is $\sim$GHz. In a frame rotating at the driving laser frequency ω_l, the Hamiltonian can then be written as (see the Appendix)

$$H = \hbar\Delta_c a^\dagger a + \hbar\Delta_d\sigma^\dagger\sigma + \hbar g(a^\dagger\sigma + a\sigma^\dagger) + \hbar\mathcal{E}\sqrt{\kappa}(a + a^\dagger) \tag{4}$$

with $\Delta_c = \omega_l - \omega_c$ and $\Delta_d = \omega_l - \omega_d$.

1077-260X/$31.00 © 2012 IEEE

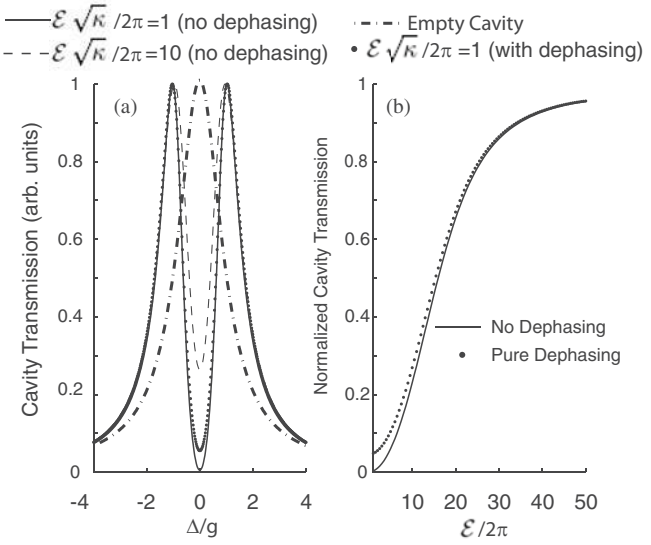

Fig. 1. DC transmission characteristics of the all-optical switch made of a strongly coupled QD-cavity system. The system is on resonance ($\omega_c = \omega_d$) and $\Delta = \Delta_c = \Delta_d$. (a) Transmission spectra for four different cases. An empty cavity shows a single Lorentzian peak. A strongly coupled QD-cavity system shows two peaks in the transmission, corresponding to the polaritons. The dip reduces both due to the pure QD dephasing, and at high laser power. The change in the dip at different driving laser power is due to the QD saturation. The units of $\sqrt{\kappa}\mathcal{E}/2\pi$ are in gigahertz. (b) Transmission on resonance with an empty cavity, i.e., at $\Delta_c = 0$ (normalized by the empty cavity transmission) as a function of the driving laser strength. For all the simulations, we assume a pure QD dephasing rate $\gamma_d/2\pi = 1$ GHz.

So far, we did not consider any loss in the system. There are two main mechanisms of loss, namely the cavity decay (with a field decay rate of κ, generally characterized by quality factor of the cavity $Q = \omega_c/2\kappa$) and the dipole spontaneous emission (with a decay rate of γ). One way to incorporate the effects of these losses is through the stochastic wave function approach [7] by simply replacing $\omega_c \rightarrow \omega_c - i\kappa$ and $\omega_d \rightarrow \omega_d - i\gamma$. The resulting frequencies corresponding to the eigenstates of such lossy system can be written as

$$\omega_{\pm} = \frac{\omega_c + \omega_d}{2} - i\frac{\kappa+\gamma}{2} \pm \sqrt{g^2 + \frac{1}{4}\left(\delta - i(\kappa-\gamma)\right)^2}. \quad (5)$$

In a strongly coupled QD-cavity system, $g > (\kappa - \gamma)/2$ and the empty cavity resonance splits into two resonances corresponding to two eigenstates of the coupled system, also known as polaritons. As a result, the transmission of a laser resonant to the empty cavity resonance decreases significantly when the cavity contains a single strongly coupled QD [see Fig. 1(a)]. However, the QD is a two-level quantum emitter and saturates with increasing power of the driving laser [see Fig. 1(b)]. This nonlinear saturation behavior is used to perform all-optical switching by the strongly coupled QD-cavity system.

The dynamics of the lossy system can be fully described using the master equation [8]

$$\frac{d\rho}{dt} = -i[H,\rho] + 2\kappa\mathcal{L}[a] + 2\gamma\mathcal{L}[\sigma] \quad (6)$$

where ρ is the density matrix of the coupled QD/cavity system. $\mathcal{L}[D]$ is the Lindbald operator corresponding to a collapse operator D. This is used to model the incoherent decays and is given by

$$\mathcal{L}[D] = D\rho D^{\dagger} - \frac{1}{2}D^{\dagger}D\rho - \frac{1}{2}\rho D^{\dagger}D. \quad (7)$$

The master equation is solved using numerical integration routines provided in quantum optics toolbox [9]. For all the simulation reported here, we used parameters observed in systems based on self-assembled QDs embedded in a photonic crystal nanocavity [5]: cavity field decay rate $\kappa/2\pi = 20$ GHz, the coherent QD-cavity interaction strength $g/2\pi = 20$ GHz, and dipole decay rate $\gamma/2\pi = 1$ GHz.

III. Semiclassical Approximation

While the approach based on the quantum optical master equation describes the behavior of the QD-cavity system precisely, the resulting numerical simulations are time consuming and require large amount of computational resources. Here, we show that, even though the switching happens at a single photon level, a semiclassical description (where we ignore the quantization of the field) describes the operation of the system quite well. Using the relation

$$\frac{d\langle D\rangle}{dt} = Tr\left[D\frac{d\rho}{dt}\right] \quad (8)$$

for any operator D, the mean-field dynamical equations for the coupled system are found to be (with the temporal profile $\mathcal{E}(t)$ for the driving laser)

$$\frac{d\langle a\rangle}{dt} = -\kappa\langle a\rangle - ig\langle\sigma\rangle - i\sqrt{\kappa}\mathcal{E}(t) \quad (9)$$

$$\frac{d\langle\sigma\rangle}{dt} = -\gamma\langle\sigma\rangle - ig\langle a\sigma_z\rangle \quad (10)$$

$$\frac{d\langle\sigma_z\rangle}{dt} = -2\gamma(\langle\sigma_z\rangle + 1) + 2ig(\langle a^{\dagger}\sigma\rangle + \langle a\sigma^{\dagger}\rangle) \quad (11)$$

where $\sigma_z = |e\rangle\langle e| - |g\rangle\langle g|$. Solving this set of equations, we need to find the dynamics of the higher order moments, namely $\langle a\sigma_z\rangle$. In the low-excitation regime, the system stays only in the lowest manifolds and we can approximate $\langle\sigma_z\rangle = -1$ and replace $\langle a\sigma_z\rangle = -\langle a\rangle$. This neglects the nonlinear nature of the QD, but matches the actual output quantitatively in the low power limit. To make the set of equations (9)–(11) a closed one, we assume $\langle a\sigma_z\rangle = \langle a\rangle\langle\sigma_z\rangle$ and $\langle a^{\dagger}\sigma\rangle = \langle a^{\dagger}\rangle\langle\sigma\rangle$. By making this approximation, we neglect the coherence of the system while analyzing the mean-field dynamical equations.

IV. Static Transmission

The switching characteristic of the all-optical switch is first calculated using a continuous wave (CW) driving laser. The cavity output $\propto \langle a^{\dagger}a\rangle$ (normalized by an empty cavity transmission) is calculated as a function of the laser power. Fig. 1 shows the nonlinear transmission characteristic of the coupled QD-cavity system. This can be thought of as the dc behavior of the switch. Fig. 1(a) shows the cavity transmission as a function of the laser frequency, for a resonant dot-cavity system (i.e., $\Delta_c = \Delta_d = \Delta$). The split resonance is a signature of the coupling between the QD and the cavity. We find that the dip

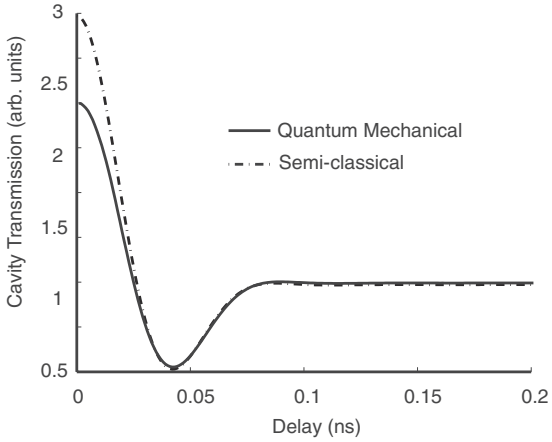

Fig. 2. Comparison between two methods: quantum optical and semiclassical. The integrated cavity transmission is plotted as a function of the delay between two pulses. The two methods match quite well at large time delay. However, they differ at the smaller time delay, as the two pulses arrive simultaneously and the total driving power is large. The parameters for simulation is $g/2\pi = 20$ GHz, $\kappa/2\pi = 20$ GHz, and $\gamma/2\pi = 1$ GHz. The pulse width is 40 ps, and the strength of the driving field is $\sqrt{\kappa}\mathcal{E}_o/2\pi = 1$ GHz. For the simulation, we assume there is no pure QD dephasing.

between the polaritons (induced by the strongly coupled QD) is reduced when the incident laser power increases. This is caused by saturation of the QD.

An important aspect of the solid-state quantum emitter is pure QD dephasing, caused by the constant interaction of the quantum emitter with the phonons in the surrounding crystal lattice [10]. This pure QD dephasing destroys the coherence of the system without affecting the population. This can be modeled by adding another Lindblad term in the master equation, $2\gamma_d \mathcal{L}(\sigma^\dagger\sigma)$. The pure QD dephasing reduces the dip in the transmission spectrum of the coupled QD-cavity system. Fig. 1(b) plots the transmission of a resonant laser through the QD-cavity system with and without pure dephasing as a function of the incident laser power. For both cases, the transmission of the system increases with increasing laser power due to saturation of the QD. However, we observe increased transmission of the laser at low power when pure dephasing is included.

V. Dynamic Switching

For any switch, the speed of switching is a very important quantity. To estimate the switching speed, we numerically calculate the dynamics of the coupled dot-cavity system. The coupled system is driven by two pulses, and the total transmission through the cavity is measured. When the two pulses are delayed by a large amount, they are transmitted through the QD-cavity system separately and we expect a constant transmission as a function of delay. However, when the pulses come closer in time, they start overlapping, and due to nonlinearity of the system, a larger transmission is expected. This can be modeled by a driving term $\mathcal{E}(t) = \mathcal{E}_c(t) + \mathcal{E}_s(t)$, where the subscripts c and s denote control and signal, respectively. For the simulations reported in this paper, we assume Gaussian envelope for both the control and the signal pulses, with a form of $\mathcal{E}_{c,s}(t) = \mathcal{E}_o \times p_{c,s}(t)$ and $p_{c,s}(t) = \exp(-\frac{(t-t_{c,s})^2}{2\sigma^2}))$, where $t_{c,s}$ denote the times of maximum amplitude for the control and the signal. Fig. 2 shows the

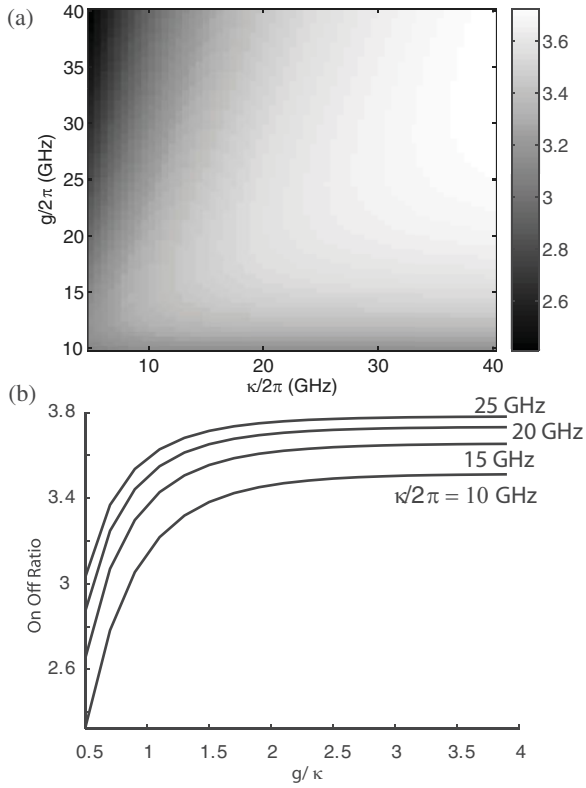

Fig. 3. (a) ON–OFF ratio (as defined in the text) under CW driving, as a function of g and κ. (b) ON–OFF ratio as a function of the ratio g/κ for different κ. An increase in on–off ratio is observed with increase in both g and κ. For this simulation, $\mathcal{E}/2\pi = 0.1$ GHz.

integrated cavity transmission as a function of delay between two pulses. This is the type of signal observed in the recently published experiments [5], [6], in which a low-speed detector was used. The two curves were obtained using the quantum optical and semiclassical approaches. As expected, the semiclassical approach is much less computationally extensive. At large delay, the two methods agree quite well, as the power of the pulses is small. However, at smaller delay, when the two pulses start to overlap, the total driving power increases, and the two methods start differing. An interesting feature in the integrated transmission of the switch is the dip that appears for small delays between the two pulses. We will explain its origin in the next paragraphs.

Next, we analyze the performance of the system as a function of the QD-cavity interaction strength g and cavity decay rate κ. In absence of any control, only signal (with a driving strength $\mathcal{E}$) interacts with the coupled system. However, in presence of a control, the total driving strength becomes $2\mathcal{E}$, assuming the control and the signal are of same strength. We define the on–off ratio of the switch as $T(2\mathcal{E})/4T(\mathcal{E})$, where $T(\mathcal{E})$ is the cavity transmission at a driving laser strength of $\mathcal{E}$. If the system is completely linear, the factor $T(2\mathcal{E})/4T(\mathcal{E})$ will always be 1. Fig. 3(a) shows the on–off ratio as a function of g and κ, maintaining the same cavity transmission for different κ. We note that the on–off ratio is not a strong function of g or κ. Fig. 3(b) shows the on–off ratio as a function of the ratio g/κ for several different values of κ. We observe that, increasing both g

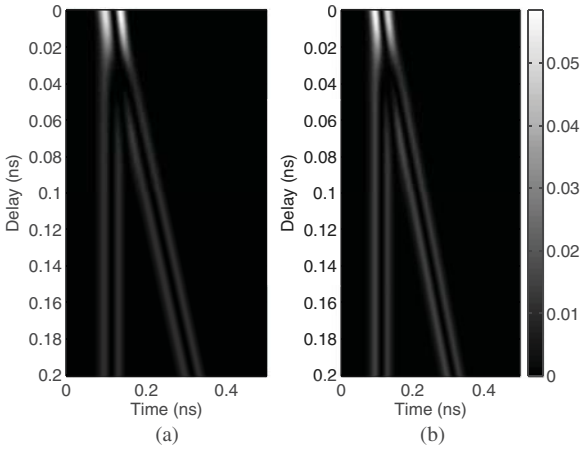

Fig. 4. Cavity transmission as a function of time (horizontal axis) when two pulses interact with the coupled QD-cavity system, for different delays between two pulses (vertical axis). We present both results obtained by (a) full quantum optical calculation and (b) semiclassically. The pulse length is 40 ps and $\sqrt{\kappa}\mathcal{E}_o/2\pi = 1$ GHz. For this weak excitation limit, the two approaches yield nearly identical results. At small delay between the two pulses, the pulses overlap, and they behave as a single pulse. At larger delay, two pulses do not meet, and propagate independently of each other. For each input pulse, we obtain two output pulses due to Rabi oscillation. At intermediate delay, there is a destructive interference between the two pulses causing reduced transmission. The parameters for simulation are $g/2\pi = 20$ GHz; $\kappa/2\pi = 20$ GHz and $\gamma/2\pi = 1$ GHz. Pure QD dephasing is neglected.

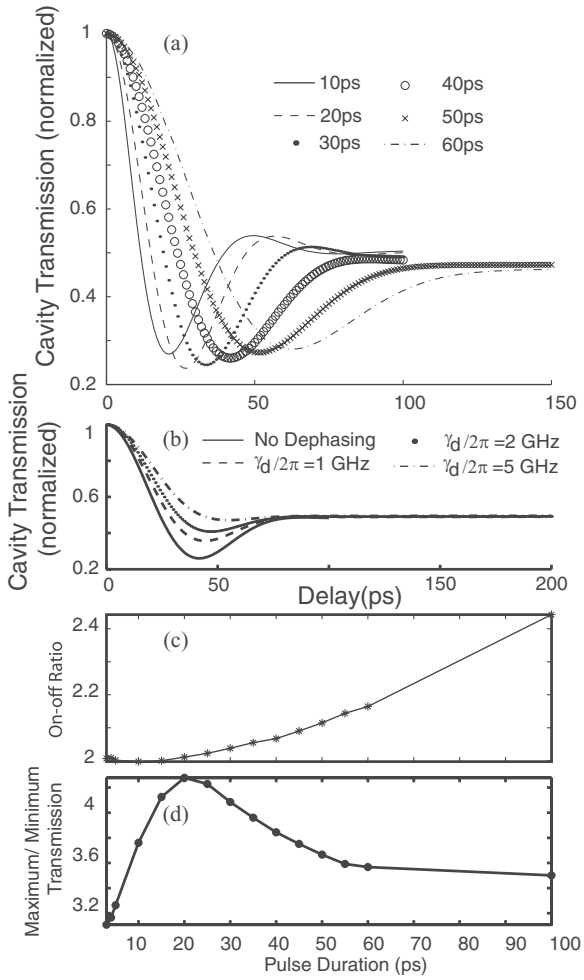

Fig. 5. Switching performance for different pulse durations. (a) Total cavity transmission integrated over time as a function of the delay between two pulses. Pulses with different pulse durations are considered in different curve. All the plots are normalized by the transmission at zero time delay. An increased transmission is observed at zero time delay. The minimum transmission at a nonzero time delay is due to a destructive interference between two pulses caused by the Rabi oscillation. (b) Effect of pure QD dephasing. With increasing QD dephasing, Rabi oscillations are suppressed, the destructive interference becomes ineffective, and the minimum transmission increases with pure QD dephasing rates. For this, a pulse width of 40 ps is assumed. (c) ON–OFF ratio (defined as the ratio of time-integrated cavity transmission between zero delay and large delay) as a function of the pulse duration. Increasing on–off ratio with increasing pulse duration is due to reduced bandwidth of the pulses. (d) Ratio between maximum and minimum transmission as a function of the pulse duration. The solid lines in (c) and (d) are just guides to the eye.

and κ improves the on–off ratio. This is because with increasing g, the separation between the two polaritons increases, which reduces the transmission of single pulses resonant with the bare cavity. On the other hand, increasing κ reduces the power needed to saturate the QD, which again causes the on—off ratio to increase.

Fig. 4(a) shows the temporal cavity output when two pulses interact with the coupled system, for different delays between the pulses for pulse duration of 40 ps. For each input pulse, we observe two pulses at the output, as can be seen from the temporal cavity output at large delay. This is a signature of Rabi oscillation between the QD and the cavity in time domain, as analyzed in [11]. We note that the semiclassical solution shown in Fig. 4(b) matches quite well with the quantum optical solution plotted in Fig. 4(a). This is expected as the simulations are performed at a low laser power. The two methods start differing at higher power, as explained in detail in [11]. This can also be seen at small time delay between two pulses, as explained previously.

Fig. 5(a) shows the integrated cavity transmission as a function of the delay between the two pulses for several pulse lengths. As expected, the highest cavity transmission is observed, when the two pulses arrive simultaneously (delay $= 0$). This is due to the saturation of the QD, which gives rise to the nonlinear behavior of the switch. When the two pulses are delayed relative to each other, the transmission of the system decreases. Numerical simulations also reveal an interesting effect of a local minimum in transmission that happens at a finite nonzero time delay. We explain this as a result of a destructive interference between the two pulses at a finite delay. We observe this effect more clearly in the temporal cavity output in Fig. 4(a). When the two pulses are temporally very close, they overlap and behave almost like a single pulse. At large delay between two pulses, the two pulses are independent of each other and we see four peaks, corresponding to two output pulses from each input pulse due to Rabi oscillation. When the delay between the two pulses matches the period of the Rabi oscillation, the second peak from the first input pulse destructively interferes with the first peak from the second input pulse. As a result, we observe only two peaks and the integrated transmission displays a local minimum [see Fig. 5(a)]. This is also supported by the fact that the width of the dip depends on the pulse duration. Increasing pure QD dephasing reduces the coherence in the system,

and causes this local minimum in the integrated transmission to eventually vanish [see Fig. 5(b)].

Next, we study the dependence of the switching performance on pulse duration. Fig. 5(c) shows the on–off ratio [defined as the ratio of the time-integrated cavity transmission at zero and large time delay, i.e., the ratio of the values in the curves in Fig. 5(a) at delay$=0$ and as delay tends to infinity)] as a function of the pulse length. We observe an increase in the on–off ratio with increasing pulse length. This is caused by the spectral bandwidth of the short pulses exceeding the width of the dip induced by the QD [see Fig. 1(a)], which results in increased transmission of single pulses. Finally, in Fig. 5(d), we examine the ratio between the maximum and minimum transmission through the coupled QD-cavity system as a function of the pulse length [practically, we plot the ratio between the maximum and minimum values of the plots in Fig. 5(a)]. The initial increase in the ratio with an increase in the pulse length can be ascribed to reduction in the pulse bandwidth. However, as the pulse length keeps increasing, complete destructive interference and cancellation of the middle peaks (see Fig. 4) cannot be achieved, which leads to a decrease in the plotted values. We note that, in this switch, we do not have a control-to-output isolation (i.e., the control goes to the output, and one cannot distinguish the control and signal), as generally required in a practical switch [12]. This can be achieved, if one has access to both the polarizations of the QD, and thus distinguishes the signal and the control by polarization. One can also use different frequencies for control and signal to separate them [13], although that might pose additional problem of cascading such switches in a network. Nevertheless, our simulation clearly shows the presence of an optical nonlinearity almost at a single photon level (i.e., at the level of a single photon in the cavity-per-cavity photon lifetime), which can be exploited to make an optical switch. As a result of imperfect in-coupling efficiency in our system, this corresponds to more than one photon outside the cavity. The coupling efficiency could be improved employing, e.g., waveguide-coupled cavity system instead of a free-space coupling to a cavity. Although in this paper we mostly analyzed switching when the signal and control are resonant to the empty cavity (i.e., the dip induced by the QD), the switching behavior is present even when they are resonant to the polaritons. Being resonant to the polaritons will also increase the coupling efficiency of the signal and control to the coupled QD-cavity system.

VI. Conclusion

We numerically analyzed the performance of the optical nonlinearity present in a strongly coupled QD-cavity system. This system can be used to perform high-speed all-optical switching at very low optical power, almost at a single photon level. A full quantum optical approach and a semiclassical approach are used to numerically simulate the operation of this system. These two approaches agree reasonably well and allow us to study in detail the temporal behavior of the switch. With current system parameters that are studied in this paper, optical switching with pulses that are several tens of picosecond in length is possible, which implies switch operation at the speed of several tens of gigahertz.

Appendix

Rotating Frame

When we switch to a frame rotating with a frequency ω_o, the new Hamiltonian $H_{\rm rot}$ becomes

$$H_{\rm rot} = T^\dagger H T + i\frac{\partial T^\dagger}{\partial t} T \tag{12}$$

where T is given by

$$T = e^{-i\omega_o t a^\dagger a} e^{-i\omega_o t \sigma^\dagger \sigma}. \tag{13}$$

The new Hamiltonian $H_{\rm rot}$ becomes

$$T^\dagger(\omega_c a^\dagger a)T = \omega_c a^\dagger a \tag{14}$$

$$T^\dagger(\omega_a \sigma^\dagger \sigma)T = \omega_a \sigma^\dagger \sigma \tag{15}$$

$$i\frac{\partial T^\dagger}{\partial t} T = -\omega_o(a^\dagger a + \sigma^\dagger \sigma) \tag{16}$$

$$T^\dagger(a)T = e^{-i\omega_o t} a \tag{17}$$

$$T^\dagger(a^\dagger)T = e^{i\omega_o t} a^\dagger \tag{18}$$

$$T^\dagger(\sigma)T = e^{-i\omega_o t} \sigma \tag{19}$$

$$T^\dagger(\sigma^\dagger)T = e^{i\omega_o t} \sigma^\dagger \tag{20}$$

$$\begin{aligned} H_{\rm rot} &= \hbar(\omega_c - \omega_o)a^\dagger a + \hbar(\omega_a - \omega_o)\sigma^\dagger \sigma \\ &\quad + \hbar g(a^\dagger \sigma + a\sigma^\dagger) + \hbar\sqrt{\kappa}\mathcal{E}(a e^{i(\omega_l - \omega_o)t} \\ &\quad + a^\dagger e^{-i(\omega_l - \omega_o)t}). \end{aligned} \tag{21}$$

Using $\omega_l = \omega_o$, the Hamiltonian in rotating frame becomes

$$H = \hbar\Delta_c a^\dagger a + \hbar\Delta_a \sigma^\dagger \sigma + \hbar g(a^\dagger \sigma + a\sigma^\dagger) + \hbar\sqrt{\kappa}\mathcal{E}(a + a^\dagger). \tag{22}$$

References

[1] H. Mabuchi, "Cavity-QED models of switches for attojoule-scale nanophotonic logic," *Phys. Rev. A*, vol. 80, pp. 045802-1–045802-4, 2009.

[2] D. Englund, A. Faraon, I. Fushman, N. Stoltz, P. Petroff, and J. Vuckovic, "Controlling cavity reflectivity with a single quantum dot," *Nature*, vol. 450, pp. 857–861, 2007.

[3] A. Faraon, A. Majumdar, H. Kim, P. Petroff, and J. Vučković, "Fast electrical control of a quantum dot strongly coupled to a photonic-crystal cavity," *Phys. Rev. Lett.*, vol. 104, pp. 047402-1–047402-4.

[4] K. Srinivasan, O. Painter, "Linear and nonlinear optical spectroscopy of a strongly coupled microdisk-quantum dot system," *Nature*, vol. 450, pp. 862–865, 2007.

[5] D. Englund, A. Majumdar, M. Bajcsy, A. Faraon, P. Petroff, and J. Vučković, "Ultrafast photon-photon interaction in a strongly coupled quantum dot-cavity system," *Phys. Rev. Lett.,* vol. 108, pp. 093604-1–093604-4, Mar. 2012.

[6] R. Bose, D. Sridharan, H. Kim, G. S. Solomon, and E. Waks, "Low-photon-number optical switching with a single quantum dot coupled to a photonic crystal cavity," *Phys. Rev. Lett.*, vol. 108, p. 227402, May 2012.

[7] C. W. Gardiner, A. S. Parkins, and P. Zoller, "Wave-function quantum stochastic differential equations and quantum jump simulation methods," *Phys. Rev. A*, vol. 46, pp. 4363–4381, 1992.

[8] H. Carmichael, Ed., *An Open Systems Approach to Quantum Optics, Lecture Notes in Physics.* Berlin, Germany: Springer-Verlag, 1993.

[9] S. M. Tan, "A computational toolbox for quantum and atomic optics," *J. Opt. B: Quantum Semiclass. Opt.*, vol. 1, no. 4, pp. 424–432, 1999.

[10] A. Majumdar, E. Kim, Y. Gong, M. Bajcsy, and J. Vučković, "Phonon mediated off-resonant quantum dot–cavity coupling under resonant excitation of the quantum dot," *Phys. Rev. B*, vol. 84, pp. 085309-1–085309-7, 2011.

[11] A. Majumdar, D. Englund, M. Bajcsy, and J. Vučković, "Nonlinear temporal dynamics of a strongly coupled quantum-dotcavity system," *Phys. Rev. A*, vol. 85, no. 3, pp. 033802-1–033802-5, Mar. 2012.
[12] D. Miller, "Are optical transistors the logical next step?," *Nature Photon.*, vol. 4, pp. 3–5, 2010.
[13] I. Fushman, D. Englund, A. Faraon, N. Stoltz, P. Petroff, and J. Vuckovic, "Controlled phase shifts with a single quantum dot," *Science*, vol. 320, pp. 769–772, 2008.

Arka Majumdar received the B.Tech. (Hons.) degree from the Indian Institute of Technology Kharagpur, Kharagpur, India, and the M.S. degree in electrical engineering from Stanford University, Stanford, CA.

He is currently a graduate student at Stanford University. His research interests include solid-state nanophotonics, quantum optics, and physics of new interconnects.

Mr. Majumdar is the recipient of President's (of India) Gold Medal from the Indian Institute of Technology, and Stanford Graduate Fellowship from Stanford University.

Michal Bajcsy received the Ph.D. degree in applied physics from Harvard University, Cambridge, MA, in 2010.

He is currently a Postdoctoral Scholar at Stanford University, Stanford, CA. His research interests include quantum optics with atoms and solid-state microcavities.

Dirk Englund received the Ph.D. degree in applied physics from Stanford University, Stanford, CA, in 2009.

He is currently an Assistant Professor at Columbia University, New York.

Jelena Vučković received the Ph.D. degree from the California Institute of Technology, Pasadena, in 2002.

She is currently an Associate Professor and a Chambers Faculty Scholar at Stanford University, Stanford, CA, where she is involved in research on experimental nanophotonics and quantum photonics.

Dr. Vučković is the recipient of several awards, including the Humboldt Prize, the Presidential Early Career Award for Scientists and Engineers, the Office of Naval Research Young Investigator Award, and the Defense Advanced Research Projects Agency Young Faculty Award.